CHALMERS
UNIVERSITY OF TECHNOLOGY

Packet Reception Probabilities in Vehicular Communications Close to Intersections

Packet Reception Probabilities in Vehicular Communications Close to Intersections

Erik Steinmetz, Matthias Wildemeersch *Member, IEEE*, Tony Q.S. Quek, *Fellow, IEEE*, and Henk Wymeersch, *Member, IEEE*

***Abstract*—Vehicular networks allow vehicles to share information and are expected to be an integral part of future intelligent transportation systems (ITS). To guide and validate the design process, analytical expressions of key performance metrics such as packet reception probabilities and throughput are necessary, in particular for accident-prone scenarios such as intersections. In this paper, we present a procedure to analytically determine the packet reception probability and throughput of a selected link, taking into account the red relative increase in the number of vehicles (i.e., possible interferers) close to an intersection. We consider both slotted Aloha and CSMA/CA MAC protocols, and show how the procedure can be used to model different propagation environments of practical relevance. The procedure is validated for a selected set of case studies at low traffic densities.**

I. Introduction

VEHICULAR networks have gained considerable attention in the past years and are regarded as one of the key components in future intelligent transportation systems (ITS) [2]. By the use of wireless communication, they allow vehicles to continuously share information with each other and their surrounding (e.g., roadside infrastructure) to perceive potentially dangerous situations in an extended space and time horizon [3]. The IEEE 802.11p standard has been defined to meet the communication demand of ITS applications, and 5G cellular networks standards are being developed to support device-to-device (D2D) communication [4]. However, different ITS applications clearly have different requirements on the communication links, with the most stringent demands imposed by safety-related applications, with extremely low latencies (below 50 ms in pre-crash situations), high delivery ratios (for full situational awareness), and relatively long communication ranges (to increase the time to react in critical situations) [5]–[7]. These requirements, in combination with a possible high density of vehicles, makes the design of vehicular communication systems challenging. This is further exacerbated by high mobility and passing vehicles, which leads to rapidly changing signal propagation conditions (including both severe multipath and shadowing) and constant topology changes. A large body of research exists in the area of vehicular communication [2], though few deal specifically with intersections. Recent propagation studies have revealed that there are complex dependencies of the received power based on the absolute positions of transmitter and receiver, the widths of the roads, and different loss exponents for own and orthogonal road [8], [9]. Studies at the physical [10] and MAC [11], [12] layer have turned to simulations to evaluated performance. To guide and validate the communication system design, measurements are often used [7], [13] to complement simulations, though both are time consuming and scenario-specific. Thus, to faster obtain insight in scalability and performance, analytical expressions of key performance metrics are necessary. Especially for high velocity scenarios (in particular highways) and accident-prone scenarios (e.g., intersections). Stochastic geometry is a tool to obtain such expressions and has been widely used in the design and analysis of wireless networks [14].

In 2-D planar networks, stochastic geometry is a mature methodology for performance evaluation in the presence of interference. Approaches to consider both geographical and medium access control (MAC) induced clustering [15], [16] and different types of fading [17]–[19] exist. In vehicular networks, where the location of the nodes are restricted by the roads, a number of studies have focused on one-dimensional topologies [20]–[23], generally preserving the spatial homogeneity also present in 2-D planar networks. For these vehicular scenarios, geographical clustering has been addressed in [20], while effects due to the 802.11p carrier sense multiple access (CSMA) MAC protocol were studied in [21], [22], [24], [25]. Besides this, [25] have studied multi-hop transmissions in a multi-lane highway scenario. These works thus enable communication system analysis for highway scenarios, but do not capture well the salient effects of intersections. This includes specific propagation characteristics and performance dependent on the position of transmitter and receiver, rather than their Euclidean distance. Intersections were considered explicitly in [1], [26], [27], which found that it is important to properly model the interference from different roads and account for the distance of receivers to the intersection, i.e., to take into account the relative increase in the number of possible interferers in the intersection due to the crossing of roads.

In this paper, we present a procedure for the evaluation of packet reception probability and throughput in intersection

E. Steinmetz and H. Wymeersch are with the Department of Electrical Engineering, Chalmers University of Technology, Gothenburg, Sweden, e-mails: {estein,henkw}@chalmers.se. E. Steinmetz is also with RISE Research Institutes of Sweden, Borås, Sweden. M. Wildemeersch is with the International Institute for Applied Systems Analysis (IIASA), Laxenburg, Austria, e-mail: wildemee@iiasa.ac.at. T.Q.S. Quek is with Singapore University of Technology and Design, Singapore, e-mail: tonyquek@sutd.edu.sg. This research was supported, in part, by the National Metrology Institute hosted at RISE Research Institutes of Sweden, which in turn is partly funded by VINNOVA under the program for national metrology (project 2015-06478); the European Research Council under Grant No. 258418 (COOPNET) and the EU project HIGHTS (High precision positioning for cooperative ITS applications) MG-3.5a-2014-636537. Part of this work was presented in [1].

scenarios and provide a model repository that can be used to adapt to a variety of different environments of importance in the vehicular context. This includes both rural and urban scenarios, different propagation conditions, and different MAC protocols. Through numerical simulations, we have verified our analytical results under the considered assumptions. We have also analyzed the performance under model mismatch through a microscopic traffic simulator SUMO (Simulation of Urban MObility) [28]. We found that under model mismatch, the analytical results deviate from the simulations, especially in dense traffic. The main difference with respect to our previous works [1], [26], [27] is as follows: our preliminary work [1] developed several basic concepts for a single scenario (rural, Aloha), but not the current framework; [26] employed the same scenario as [1], but considered the special case of a central node near the intersection; [27] extended the path loss model to urban intersections, but was limited to Aloha and Rayleigh fading. The current paper goes beyond these three works and provides a novel procedure, complemented with simulations in a number of selected case studies.

II. System Model

A. Scenario

We consider an intersection scenario with two perpendicular roads, as shown in Fig. 1. We assume that the width of the two roads[1] indicated by H and V can be neglected, and that the roads each carry a stream of vehicles, modeled as one-dimensional homogeneous Poisson point processes (PPPs). The intensity of vehicles on both roads is denoted by λ_{H} and λ_{V}, and the point processes describing the location of the vehicles on the two roads are represented by $\Phi_{\mathrm{H}} \sim \mathrm{PPP}(\lambda_{\mathrm{H}})$ and $\Phi_{\mathrm{V}} \sim \mathrm{PPP}(\lambda_{\mathrm{V}})$. The positions of individual vehicles (also referred to as nodes) on the two roads H and V are denoted by $\mathbf{x}_i = [x_i, 0]^{\mathrm{T}}$ and $\mathbf{x}_i = [0, y_i]^{\mathrm{T}}$, respectively, assuming the roads are aligned with the horizontal and vertical axes. We consider a transmitter (Tx) with location[2] $\mathbf{x}_{\mathrm{tx}} = [x_{\mathrm{tx}}, y_{\mathrm{tx}}]^{\mathrm{T}}$, which broadcasts with a fixed transmission power P. The receiver (Rx) is assumed to be a distance d away from the intersection on either the H- or V-road, such that the location is either $\mathbf{x}_{\mathrm{rx}} = [x_{\mathrm{rx}}, 0]^{\mathrm{T}}$ or $\mathbf{x}_{\mathrm{rx}} = [0, y_{\mathrm{rx}}]^{\mathrm{T}}$. The signal propagation comprises power fading S and path loss $l(\mathbf{x}_{\mathrm{tx}}, \mathbf{x}_{\mathrm{rx}})$. At the Rx, the signal is further affected by white Gaussian noise with noise power N and interference from other concurrently transmitting vehicles on the H- and V-road. The amount of interference experienced by the Rx depends on the choice of MAC protocol. For a given MAC scheme, the position of interfering vehicles at a given time can be represented by the thinned point processes $\Phi_{\mathrm{H}}^{\mathrm{MAC}}$ and $\Phi_{\mathrm{V}}^{\mathrm{MAC}}$.[3] We can express the signal-to-interference-plus-noise ratio (SINR) as

$$\mathrm{SINR} = \frac{P\, S_0 l(\mathbf{x}_{\mathrm{tx}}, \mathbf{x}_{\mathrm{rx}})}{\sum_{\mathbf{x} \in \Phi_{\mathrm{H}}^{\mathrm{MAC}} \cup \Phi_{\mathrm{V}}^{\mathrm{MAC}}} P\, S_{\mathbf{x}} l(\mathbf{x}, \mathbf{x}_{\mathrm{rx}}) + N} \qquad (1)$$

[1]The generalization to multiple roads and multiple lanes is straightforward in most cases.

[2]Note that the Tx can belong to either Φ_{H} or Φ_{V} (but does not necessarily have to) as the results still hold due to Slivnyak's Theorem [14, Theorem A.5]

[3]For a general MAC scheme, the thinned process is not necessarily homogeneous.

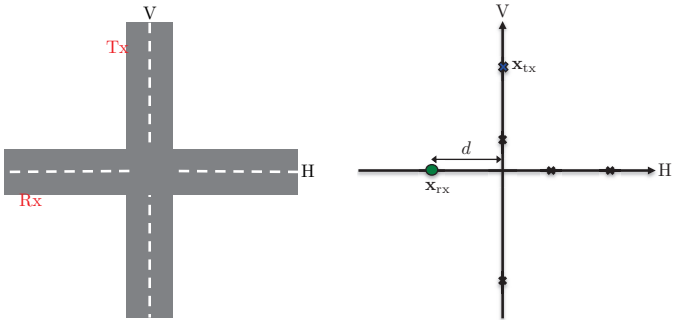

(a) intersection scenario (b) abstraction

Fig. 1. Illustration of considered scenario: (a) A two-way intersection scenario in which each road carries a stream of vehicles, (b) the abstraction used in modeling. The Tx (indicated by the blue car) can be at any location, while the target Rx (green car) can be located on either the H- or V-road. Other vehicles on the roads H and V, of which some transmit concurrently and cause interference, are shown as gray cars.

where S_0 denotes the fading on the useful link and $S_{\mathbf{x}}$ denotes the fading on an interfering link for an interferer at location $\mathbf{x}$. A packet is considered to be successfully received if the SINR exceeds a threshold β.

Our aim is to analytically characterize (i) the probability that the Rx successfully receives a packet sent by the Tx; (ii) the throughput of the link between Tx and Rx. This problem is challenging due to the specific propagation conditions and interference levels experienced in these intersection scenarios. In the next section, we will describe these in more detail.

B. Models in Vehicular Communication

In this section, we discuss characteristics for vehicular channels that are important from an SINR point of view, and detail different models regarding path loss, fading, and MAC protocol.

1) Power Decay and Blockage: Extensive measurement campaigns [7]–[9], [29], [30] have been performed to characterize the vehicular channel in a variety of propagation environments such as rural, highway, suburban, and urban scenarios. We will distinguish between line-of-sight (LOS) and non-line-of-sight (NLOS) propagation, depending on whether or not the direct LOS signal between a Rx and a Tx is blocked. For LOS propagation, conventional path loss models, where power decays approximately with the squared Euclidean distance between Rx and Tx are well-accepted [7]: $l_{\mathrm{E}}(\mathbf{x}_{\mathrm{tx}}, \mathbf{x}_{\mathrm{rx}}) = A \left\| \mathbf{x}_{\mathrm{rx}} - \mathbf{x}_{\mathrm{tx}} \right\|_2^{-\alpha}$, where $\|\cdot\|_2$ is the ℓ_2 norm, $\alpha > 0$ is the path loss exponent, and A is a constant that depends on several factors such as antenna characteristics, carrier frequency, and propagation environment. For NLOS propagation, e.g., in urban canyons, measurements indicate increased loss over LOS propagation, with complex dependencies on the absolute position of Tx and Rx, widths of the roads, and different loss exponents for own and orthogonal road [8], [9]. The complexity of these models renders them intractable when it comes to mathematical analysis, so we rely on the simpler and more tractable Manhattan model, which was first proposed for modeling of similar scenarios in the well-known WINNER II project [31]: $l_{\mathrm{M}}(\mathbf{x}_{\mathrm{tx}}, \mathbf{x}_{\mathrm{rx}}) = A \left\| \mathbf{x}_{\mathrm{rx}} - \mathbf{x}_{\mathrm{tx}} \right\|_1^{-\alpha}$,

where $\|\cdot\|_1$ is the ℓ_1 norm, and the values of α and A might be different from the LOS case. It has been shown that typical path loss exponents for the vehicular channel are in the range 1.6-2.1 [7], [30].

2) Random Power Variations Due to Fading : Fading refers to random fluctuations in the received power around the average received power, given by the path loss. The fading experienced on a link depends on the scenario and the environment and is typically modeled as a random variable [32]. For rural LOS links, exponential fading is considered an appropriate model [9], [33], while for urban NLOS link, a log-normal model [8], [9] with power variations of 3–6 dB have been found to be appropriate.

3) MAC Protocols: The MAC protocol governs when a user can access the channel and aims to control the interference in the network. Two common MAC protocols for ad-hoc networks are slotted Aloha and CSMA with collision avoidance (CSMA/CA). In slotted Aloha, which is the simpler of the two, nodes that have a packet to send, access the channel during a time slot with a probability $p \in [0,1]$. In contrast, in CSMA/CA, before sending a packet, a node verifies that the channel is free by listening to the channel. Only if the channel is free, the node transmits the packet. If the channel is busy, the node is forced to wait a random back-off time before it can try again [13]. Even though CSMA/CA always results in a better throughput vs load performance, CSMA/CA and slotted Aloha have been shown to exhibit similar performance in terms of outage probability for dense one-dimensional scenarios [21], [24]. In this paper we will consider both slotted Aloha and CSMA/CA, where the latter of these two MAC protocols is the one used in the 802.11p standard designed for the first generation vehicular networks.

III. Stochastic Geometry Analysis

In this section, we describe a unified methodology to compute the communication performance for all these conditions, as well as different MAC protocols. In particular, we will determine (i) the packet reception probability $\mathbb{P}(\beta, \mathbf{x}_{\rm rx}, \mathbf{x}_{\rm tx})$, i.e., the probability that a receiver located at $\mathbf{x}_{\rm rx}$ can successfully decode a transmission from a transmitter located at $\mathbf{x}_{\rm tx}$, in the presence of interferers on the H- and V-road; (ii) the throughput $\mathcal{T}(\beta, \mathbf{x}_{\rm rx}, \mathbf{x}_{\rm tx})$, i.e., the expected rate for the link between the Rx and Tx at locations $\mathbf{x}_{\rm rx}$ and $\mathbf{x}_{\rm tx}$, accounting for both the packet reception probability and the probability of gaining access to the channel. Both $\mathbb{P}(\beta, \mathbf{x}_{\rm rx}, \mathbf{x}_{\rm tx})$ and $\mathcal{T}(\beta, \mathbf{x}_{\rm rx}, \mathbf{x}_{\rm tx})$ depend on the loss function, fading distribution, and the MAC protocol. Note that the loss function and fading distribution relate to the power decay and blockage as well as the random signal variations in the specific scenario, while the MAC protocol relates to number of interferers and their locations. Several applications of this methodology will be discussed in Section IV.

A. Packet Reception Probability

To derive the packet reception probability for the intersection scenario, we start by accounting for the fading distribution of the useful link. We express

$$\begin{aligned}\mathbb{P}(\beta, \mathbf{x}_{\rm rx}, \mathbf{x}_{\rm tx}) &= \Pr(\mathrm{SINR} \geq \beta) \\ &= \Pr\left(S_0 \geq \left(I_{\rm H} + I_{\rm V} + \tilde{N}\right)\beta / l(\mathbf{x}_{\rm tx}, \mathbf{x}_{\rm rx})\right) \end{aligned} \tag{2}$$

in which $\tilde{N} = N/P$ and $I_{\rm H} = \sum_{\mathbf{x}\in\Phi_{\rm H}^{\rm MAC}} S_{\mathbf{x}} l(\mathbf{x}, \mathbf{x}_{\rm rx})$ while $I_{\rm V} = \sum_{\mathbf{x}\in\Phi_{\rm V}^{\rm MAC}} S_{\mathbf{x}} l(\mathbf{x}, \mathbf{x}_{\rm rx})$. Conditioning on the path loss, we can now write the packet reception probability as

$$\begin{aligned}&\mathbb{P}(\beta, \mathbf{x}_{\rm rx}, \mathbf{x}_{\rm tx}) \\ &= \mathbb{E}_{I_{\rm H}, I_{\rm V}}\left\{\bar{F}_{S_0}\left(\left(I_{\rm H} + I_{\rm V} + \tilde{N}\right)\beta / l(\mathbf{x}_{\rm tx}, \mathbf{x}_{\rm rx})\right)\right\} \\ &= \iint \bar{F}_{S_0}\left(\left(t_1 + t_2 + \tilde{N}\right)\tilde{\beta}\right) f_{I_{\rm H}, I_{\rm V}}(t_1, t_2)\mathrm{d}t_1\mathrm{d}t_2,\end{aligned} \tag{3}$$

where $\tilde{\beta} = \beta / l(\mathbf{x}_{\rm tx}, \mathbf{x}_{\rm rx})$, $f_{I_{\rm H}, I_{\rm V}}(t_1, t_2)$ is the interference distribution, and $\bar{F}_{S_o}(s_0)$ is the complementary cumulative distribution function (CCDF) of the random variable S_0, evaluated in s_0.

The expression (3) can be interpreted in two ways: (i) as the expectation of $\bar{F}_{S_0}((I_{\rm H} + I_{\rm V} + \tilde{N})\beta / l(\mathbf{x}_{\rm tx}, \mathbf{x}_{\rm rx}))$ with respect to the interference distribution; and (ii) as the transformation of the interference distribution with a kernel function determined by the CCDF of the fading distribution of the useful link. In either interpretation, the distributions of the interference and the fading play an important role. Note that for all relevant fading distributions of the useful link, (3) will result in the Laplace transform (LT) of the interference distribution or a function of LTs of the interference distribution. It is therefore convenient to express these distributions through their LT or, equivalently, their moment generating function (MGF).

1) LT of the Interference: For Aloha, the interference distribution factorizes $f_{I_{\rm H}, I_{\rm V}}(t_1, t_2) = f_{I_{\rm H}}(t_1) f_{I_{\rm V}}(t_2)$, while for CSMA/CA, the interference from the H- and V-road are not independent. We will however approximate it as being independent, using a location dependent thinning of the original PPPs [34], as described in Section III-A3. Hence, we can focus on a single road ${\rm R} \in \{{\rm H}, V\}$, with interference distribution $f_{I_{\rm R}}$. The Laplace transform of $f_{I_{\rm R}}$ is defined as

$$\mathcal{L}_{I_{\rm R}}(s) = \mathbb{E}[\exp(-sI_{\rm R})], \tag{4}$$

in which

$$I_{\rm R} = \sum_{\mathbf{x}\in\Phi_{\rm R}^{\rm MAC}} S_{\mathbf{x}} l(\mathbf{x}, \mathbf{x}_{\rm rx}). \tag{5}$$

Substitution of (5) into (4) then yields

$$\mathcal{L}_{I_{\rm R}}(s) \overset{(a)}{=} \mathbb{E}_{\Phi}\left[\prod_{\mathbf{x}\in\Phi_{\rm R}^{\rm MAC}} \mathbb{E}_{S_{\mathbf{x}}}\left\{\exp\left(-s\, S_{\mathbf{x}} l(\mathbf{x}, \mathbf{x}_{\rm rx})\right)\right\}\right] \tag{6}$$

$$= \mathbb{E}_{\Phi}\left[\prod_{\mathbf{x}\in\Phi_{\rm R}^{\rm MAC}} \mathcal{L}_{S_{\mathbf{x}}}\left(s\, l(\mathbf{x}, \mathbf{x}_{\rm rx})\right)\right] \tag{7}$$

$$\overset{(b)}{=} \exp\Bigg(-\int_{-\infty}^{+\infty} \lambda_{\rm R}^{\rm MAC}\left(\mathbf{x}\left(z\right), \mathbf{x}_{\rm tx}\right) \times \left(1 - \mathcal{L}_{S_{\mathbf{x}}}\left(s\, l(\mathbf{x}(z), \mathbf{x}_{\rm rx})\right)\right) \mathrm{d}z\Bigg), \tag{8}$$

where (a) holds due to the independence of the fading parameters, $\mathbb{E}_{\Phi}[\cdot]$ is the expectation operator with respect to the

location of the interferers, and $\mathcal{L}_{S_{\mathbf{x}}}(\cdot)$ is the LT of the fading distribution of the interfering link; (b) is due to the probability generating functional (PGFL) for a PPP [14, Definition A.5], in which $\lambda_{\mathrm{R}}^{\mathrm{MAC}}(\mathbf{x}(z), \mathbf{x}_{\mathrm{tx}})$ represents the intensity of the PPP $\Phi_{\mathrm{R}}^{\mathrm{MAC}}$, which depends on the specific MAC protocol and in some cases on the transmitter's location. Note that in (8), the intensity is defined over $z \in \mathbb{R}$, which represents the position along the road $\mathrm{R} \in \{\mathrm{H}, V\}$, where $\mathbf{x}(z) = [z\,0]^{\mathrm{T}}$ when $\mathrm{R} = \mathrm{H}$ and $\mathbf{x}(z) = [0\,z]^{\mathrm{T}}$ when $\mathrm{R} = V$. To determine $\mathcal{L}_{I_{\mathrm{R}}}(s)$, we must be able to compute the integral (8), which involves knowledge of $\lambda_{\mathrm{R}}^{\mathrm{MAC}}(\mathbf{x}(z), \mathbf{x}_{\mathrm{tx}})$ and $\mathcal{L}_{S_{\mathbf{x}}}(s)$.

Remark 1. The Laplace transform of the interference can also be computed using the principle of stochastic equivalence [19], where the LT in case of an arbitrary fading distribution can be found based on the LT in case of Rayleigh fading, given an appropriate scaling of the system parameters.

2) LT of Fading: For many relevant fading distributions, the LT is known, including for exponential, Gamma, Erlang, and χ^2 random variables. While the log-normal distribution is harder to deal with, it can be approximated by the Erlang distribution [35], which combines tractability with expressiveness. When $S_{\mathbf{x}} \sim \mathrm{E}(k, \theta)$, i.e., an Erlang distribution with shape parameter $k \in \mathbb{N}$ and rate parameter $1/\theta > 0$, then

$$\mathcal{L}_{S_{\mathbf{x}}}(s) = (1 + s\theta)^{k}. \tag{9}$$

As special cases, (i) $k = 1$ corresponds to an exponential distribution with mean θ; (ii) $\theta = 1/k$ corresponds to Nakagamim power fading.

3) Intensity of the Interfering PPPs: The intensity $\lambda_{\mathrm{R}}^{\mathrm{MAC}}(\mathbf{x}(z), \mathbf{x}_{\mathrm{tx}})$ of the interference depends on the type of MAC that is utilized. We distinguish between two cases: slotted Aloha with transmit probability $p \in [0, 1]$, and CSMA/CA with interference region with range $\delta \geq 0$ (i.e., interference can be sensed up to δ meters). For a slotted Aloha MAC, vehicles transmit with probability p independently of each other. Thus, we have an independent thinning of $\Phi_{\mathrm{R}} \sim \mathrm{PPP}(\lambda_{\mathrm{R}})$, such that $\lambda_{\mathrm{R}}^{\mathrm{MAC}}(\mathbf{x}(z), \mathbf{x}_{\mathrm{tx}}) = p\lambda_{\mathrm{R}}$, irrespective of the position along the road $\mathbf{x}(z)$ and the transmitter location $\mathbf{x}_{\mathrm{tx}}$.

For a CSMA/CA MAC, a vehicle will transmit if it has the lowest random timer within its sensing range (interference region). This means that (i) the intensity is a function of $\mathbf{x}_{\mathrm{tx}}$ as other nodes in its interference region are forced to be silent when it is active; (ii) the interference from the H- and V-road is not independent. The timer process and the corresponding dependent thinning result in a MatÃ©rn hard-core process type II, which can be approximated by a PPP with independently thinned node intensity. The approximation of the hard-core process by a PPP is shown to be accurate in [34] and has been applied in the context of heterogeneous cellular networks, for instance in [36].[4] When the transmitter at $\mathbf{x}_{\mathrm{tx}}$ is active the resulting intensity of the PPPs used to approximate the point process of interferers can be expressed as

$$\lambda_{\mathrm{R}}^{\mathrm{MAC}}(\mathbf{x}(z), \mathbf{x}_{\mathrm{tx}}) = \begin{cases} p_A(\mathbf{x}(z))\,\lambda_{\mathrm{R}} & \|\mathbf{x}(z) - \mathbf{x}_{\mathrm{tx}}\| > \delta \\ 0 & \|\mathbf{x}(z) - \mathbf{x}_{\mathrm{tx}}\| \leq \delta. \end{cases} \tag{10}$$

In (10), $p_A(\mathbf{x}(z))$ is the access probability of a node. The access probability (which is used to thin the original process) is the probability that the given node has the smallest random timer in the corresponding interference region (in this case modeled as a 2-dimensional ball $\mathcal{B}_2(\mathbf{x}(z), \delta)$ with range δ centered at location $\mathbf{x}(z)$), and can for one of the roads be expressed as

$$p_A(\mathbf{x}(z)) = \int_0^1 \exp(-t\Lambda(\mathcal{B}_2(\mathbf{x}(z), \delta)))\mathrm{d}t \tag{11}$$

$$= \frac{1 - \exp(-\Lambda(\mathcal{B}_2(\mathbf{x}(z), \delta)))}{\Lambda(\mathcal{B}_2(\mathbf{x}(z), \delta))}, \tag{12}$$

where

$$\Lambda(\mathcal{B}_2(\mathbf{x}(z), \delta)) = \begin{cases} 2\delta\lambda_{\mathrm{R}} & \|\mathbf{x}(z)\| > \delta \\ 2\delta\lambda_{\mathrm{R}} + 2\sqrt{\delta^2 - \|\mathbf{x}(z)\|^2}\lambda_{\mathrm{R}'} & \|\mathbf{x}(z)\| \leq \delta \end{cases} \tag{13}$$

represents the average number of nodes in the interference region. Note that the average number of nodes, and thus the access probability depends on the position z along the road and the intensities λ_{R} and $\lambda_{\mathrm{R}'}$, which here represent the intensities of the unthinned processes on the relevant road R and the other road, respectively. Approximating CSMA/CA via a non-homogeneous PPP does not capture certain effects such as listen-before-talk errors or MAC extensions such as clear channel assessment (CCA) threshold adaptation, but instead aims to generate the resulting interference.

B. Throughput

From a system perspective, the packet reception probability is not sufficient to characterize the performance, since a MAC that allows few concurrent transmissions leads to high packet reception probabilities but low throughputs. Thus, to be able to compare the impact of different MAC protocols, we characterize the throughput for the intersection scenario, i.e., the number of bits transmitted per unit time and bandwidth on a specific link. For the case with a receiver and transmitter located at $\mathbf{x}_{\mathrm{rx}}$ and $\mathbf{x}_{\mathrm{tx}}$, respectively, we express the throughput as

$$\mathcal{T}(\beta, \mathbf{x}_{\mathrm{rx}}, \mathbf{x}_{\mathrm{tx}}) = p_A(\mathbf{x}_{\mathrm{tx}})\mathbb{P}(\beta, \mathbf{x}_{\mathrm{rx}}, \mathbf{x}_{\mathrm{tx}}) \log_2(1 + \beta) \tag{14}$$

where $p_A(\mathbf{x}_{\mathrm{tx}})$ is the access probability of a transmitter located at $\mathbf{x}_{\mathrm{tx}}$, i.e., the probability that the transmitter obtains access to the channel to transmit a packet. For the slotted Aloha MAC, the access probability is simply $p_A(\mathbf{x}_{\mathrm{tx}}) = p$, while for the CSMA/CA case the access probability is given in (12) and depends on the void probability in the 2-dimensional ball used to model the interference region around $\mathbf{x}_{\mathrm{tx}}$.

[4]The extension to CSMA/CA schemes with discrete back-off timers has been proposed in [21], which retains concurrent transmitters due to the non-zero probability of nodes with the same timer value.

C. Procedure

Given the analysis in the previous subsections, the procedure for determining the packet reception probability $\mathbb{P}(\beta, \mathbf{x}_{\rm rx}, \mathbf{x}_{\rm tx})$ and the throughput $\mathcal{T}(\beta, \mathbf{x}_{\rm rx}, \mathbf{x}_{\rm tx})$ is thus as follows: (i) Determine the fading LT $\mathcal{L}_{S_{\mathbf{x}}}(s)$ for the interfering links, as described in Section III-A2; (ii) Determine the intensity of the interference PPP $\lambda_{\rm R}^{\rm MAC}(\mathbf{x}(z), \mathbf{x}_{\rm tx})$ for ${\rm R} \in \{{\rm H}, {\rm V}\}$, as described in Section III-A3; (iii) From steps (i) and (ii), determine the LT of the interference $\mathcal{L}_{I_{\rm R}}(s)$ for ${\rm R} \in \{{\rm H}, {\rm V}\}$ using (8); (iv) Determine the fading LT $\mathcal{L}_{S_0}(s)$ for the useful link, as described in Section III-A2; (v) From steps (iii) and (iv), determine $\mathbb{P}(\beta, \mathbf{x}_{\rm rx}, \mathbf{x}_{\rm tx})$ using (3), either by drawing samples from the interference (using standard techniques, given the interference distribution characterized through its LT), or by considering the CCDF of the fading on the useful link as a kernel in a transformation (i.e., evaluating a function of LTs of the interference distribution). Finally, use the obtained packet reception probability $\mathbb{P}(\beta, \mathbf{x}_{\rm rx}, \mathbf{x}_{\rm tx})$ in conjunction with the access probability $p_A(\mathbf{x}_{\rm tx})$ used in step (ii) to determine the throughput $\mathcal{T}(\beta, \mathbf{x}_{\rm rx}, \mathbf{x}_{\rm tx})$. Whether or not each step is tractable depends on the assumptions we make regarding the loss function, the fading distribution, and the MAC protocol, which will be further discussed in Section IV.

IV. Case Studies

In this Section we present three case studies to show how the different models presented in the paper can be used to model both rural and urban intersection scenarios, and how shadowing, LOS blockage, and different MAC protocols affect the performance of the communication system.

A. Case I - Rural Intersection with Slotted Aloha

In the rural intersection scenario [1], [26], vehicles are assumed to communicate via LOS links. Hence, path loss is described by the Euclidean distance loss function $l_{\rm E}(\cdot)$, with path loss exponent $\alpha = 2$, while power fading is modeled with an exponential distribution (i.e., $S \sim E[1,1]$), for both useful and interfering links. Furthermore, we consider a slotted Aloha MAC with transmit probability p. Using the procedure from Section III-C, the packet reception probability for the rural intersection scenario is given in Proposition 2 (see also [1], [26]).

Proposition 2. *Given a slotted Aloha MAC with transmit probability p, exponential fading (i.e, $S \sim E(1,1)$) for each link, Euclidean loss function $l_{\rm E}(\cdot)$ with path loss exponent $\alpha = 2$, and a scenario as outlined in Section II, the packet reception probability can be expressed as*

$$\begin{aligned}\mathbb{P}(\beta, \mathbf{x}_{\rm rx}, \mathbf{x}_{\rm tx}) = \exp\left(-\frac{N\beta\left\|\mathbf{x}_{\rm rx}-\mathbf{x}_{\rm tx}\right\|_2^2}{PA}\right) \\ \times \exp\left(-p\lambda_{\rm H}\pi\sqrt{\beta}\left\|\mathbf{x}_{\rm rx}-\mathbf{x}_{\rm tx}\right\|_2\right) \\ \times \exp\left(-\frac{p\lambda_{\rm V}\pi\beta\left\|\mathbf{x}_{\rm rx}-\mathbf{x}_{\rm tx}\right\|_2^2}{\sqrt{\beta\left\|\mathbf{x}_{\rm rx}-\mathbf{x}_{\rm tx}\right\|_2^2+d^2}}\right)\end{aligned} \tag{15}$$

Proof: The proof follows from applying the approach from III-C and is a special case of [37]. ∎

We note that the packet reception probability comprises three factors: the first factor corresponds to the packet reception probability in the absence of interferers; the second factor captures the reduction of the packet reception probability due to interferers on the H-road; the third factor captures the additional reduction of packet reception probability due to interferers on the V-road.

Remark 3. As was noted in [1], it is possible to extend Proposition 2 to a scenario with additional roads/lanes with arbitrary orientations, each road contributing with an additional factor to the packet reception probability. This approach can, for example, be used to take into account interference from surrounding roads. Furthermore, it can be used to handle cases where the width of the roads can no longer be ignored, by splitting the road into several lanes.

B. Case II - Urban Intersection with Slotted Aloha

This case study models an urban intersection scenario with the Tx on the V-road and the Rx on the H-road. Signals arriving to the Rx from the V-road are assumed to be in NLOS, modeled through Manhattan path loss and Erlang fading (which serves as an approximation of log-normal fading). Signals arriving to the Rx from the own H-road are in LOS, modeled through Euclidean path loss and exponential fading. The packet reception probability for the urban intersection scenario is given in Proposition 4.

Proposition 4. *Given a slotted Aloha MAC with transmit probability p, Erlang fading (i.e., $S \sim E(k_0, \theta_0)$) and Manhattan loss function $l_{\rm M}(\cdot)$ for the useful link, Erlang fading (i.e., $S \sim E(k_V, \theta_V)$) and Manhattan loss function for the interfering links from the V-road, exponential fading (i.e, $S \sim E(1,1)$) and Euclidean loss function $l_{\rm E}(\cdot)$ for the interfering links from the H-road, and a scenario as outlined in Section II, the packet reception probability can be expressed as*

$$\mathbb{P}(\beta, \mathbf{x}_{\rm rx}, \mathbf{x}_{\rm tx}) = e^{-\frac{\zeta_N}{P}} \sum_{i=0}^{k_0-1} \sum_{j=0}^{i} \binom{i}{j} \frac{\zeta^i}{i!} C^{(j)} D^{(i-j)}, \tag{16}$$

where

$$\begin{aligned}C^{(j)} = \sum_{n=0}^{j} \binom{j}{n} \left(\frac{N}{P}\right)^{j-n} (-1)^n e^{-\kappa\sqrt{\zeta}} \zeta^{-n} \\ \times \sum_{l=0}^{n} \sum_{m=0}^{l} \frac{(-1)^m \left(-\kappa\sqrt{\zeta}\right)^l \left(\frac{2-m+l-2n}{2}\right)_n}{m!\,(-m+l)!},\end{aligned} \tag{17}$$

in which $(\cdot)_n$ is the Pochhammer symbol, $\kappa = 2p\lambda_{\rm H} A^{1/\alpha}\pi/\alpha \csc(\pi/\alpha)$, $\zeta = \beta\left\|\mathbf{x}_{\rm rx}-\mathbf{x}_{\rm tx}\right\|_1^{\alpha} / (A\theta_0)$, and $D^{(m)} = (-1)^m \frac{{\rm d}^m}{{\rm d}\zeta^m} \mathcal{L}_{I_{\rm V}}(\zeta)$.

Proof: See Appendix A. ∎

We observe that the analytical expressions become more involved when changing the loss function and the fading distribution for the links to the V-road, but in contrast to the rural intersection scenario it is possible to obtain closed form

expressions for a general α (this is because Manhattan path loss for the interferers from the V-road is easier to handle than Euclidean path loss). Furthermore, it should be noted that if the Tx is assumed to be on the H-road, the expressions become more compact (i.e., only $C^{(0)} = e^{-\kappa\sqrt{\zeta}}$ and $D^{(0)}$ remain). Moreover, similarly as for the model presented in [9], Proposition 4 only gives realistic results when the Rx and the Tx are at least a few meters away from the intersection. This is because when the Rx is at the intersection, all links become LOS, while when the Tx is at the intersection, the useful link becomes LOS. In either case, the corresponding links should be modeled with exponential fading, rather than Erlang fading.

C. Case III - Rural Intersection with CSMA/CA

In this final case study, we will focus on the MAC protocol and how it affects performance and tractability. To do this, we start from the rural intersection scenario, but replace the slotted Aloha MAC with a CSMA/CA MAC[5]. As the MAC affects not only the packet reception probability but also the access probability, we will also consider throughput in this case study. The packet reception probability for the CSMA/CA case is given in Proposition 5.

Proposition 5. *Given a CSMA/CA MAC with interference range δ, exponential fading (i.e, $S \sim E(1,1)$) for each link, Euclidean loss function $l_{\mathrm{E}}(\cdot)$ with path loss exponent $\alpha = 2$, and a scenario as outlined in Section II, the packet reception probability can be expressed as*

$$\mathbb{P}(\beta, \mathbf{x}_{\mathrm{rx}}, \mathbf{x}_{\mathrm{tx}}) = e^{-\frac{N\tilde{\beta}}{P}} \mathcal{L}_{I_{\mathrm{H}}}(\tilde{\beta}) \mathcal{L}_{I_{\mathrm{V}}}(\tilde{\beta}), \tag{18}$$

where $\tilde{\beta} = \beta / l_{\mathrm{E}}(\mathbf{x}_{\mathrm{tx}}, \mathbf{x}_{\mathrm{rx}})$, and

$$\mathcal{L}_{I_{\mathrm{H}}}(s) = \exp\left(- \int_{-\infty}^{+\infty} \frac{\lambda_{\mathrm{H}}^{\mathrm{MAC}}\left([x,0]^{\mathrm{T}}, \mathbf{x}_{\mathrm{tx}}\right)}{1 + |x_{\mathrm{rx}} - x|^2 / As} \mathrm{d}x \right) \tag{19}$$

$$\mathcal{L}_{I_{\mathrm{V}}}(s) = \exp\left(- \int_{-\infty}^{+\infty} \frac{\lambda_{\mathrm{V}}^{\mathrm{MAC}}\left([0,y]^{\mathrm{T}}, \mathbf{x}_{\mathrm{tx}}\right)}{1 + \left\|[x_{\mathrm{rx}}, -y]^{\mathrm{T}}\right\|_2^2 / As} \mathrm{d}y \right) \tag{20}$$

where $\lambda_{\mathrm{H}}^{\mathrm{MAC}}\left([x,0]^{\mathrm{T}}, \mathbf{x}_{\mathrm{tx}}\right)$ and $\lambda_{\mathrm{V}}^{\mathrm{MAC}}\left([0,y]^{\mathrm{T}}, \mathbf{x}_{\mathrm{tx}}\right)$ are given in (38) and (39), respectively.

Proof: See Appendix B ∎

As can be seen from Proposition 5, the expressions we obtain still involve an integral that can be solved numerically easily and efficiently. The throughput $\mathcal{T}(\beta, \mathbf{x}_{\mathrm{rx}}, \mathbf{x}_{\mathrm{tx}})$ is readily obtained by using the results from Proposition 5 in combination with (14).

V. Numerical Results

A. Simulation Setup

To evaluate the correctness of the above theoretical expressions, we have compared them to Monte Carlo simulation with 20,000 realizations (snapshots of the network) of the PPPs and fading parameters. We also include simulation results where the spatial distribution of vehicles is taken from a realistic simulation of a 4-way intersection with a traffic light in the SUMO traffic simulator. To make sure that the traces generated in SUMO are comparable to our analytical results the arrival process of vehicles was set such that the average number of vehicles per road matched the PPP case.[6] However, in contrast to the PPP, the vehicle motion model in SUMO in conjunction with the traffic light results in a clustering of vehicles close to the intersection. We compare both Aloha and CSMA/CA. For the purpose of visualization, we show the *outage probability* $\mathbb{P}_{\mathrm{Out}}(\beta, \mathbf{x}_{\mathrm{rx}}, \mathbf{x}_{\mathrm{tx}}) = 1 - \mathbb{P}(\beta, \mathbf{x}_{\mathrm{rx}}, \mathbf{x}_{\mathrm{tx}})$, as well as throughput. The intensity of vehicles on the two roads are $\lambda_{\mathrm{H}} = \lambda_{\mathrm{V}} = 0.01$ (i.e., with an average inter-vehicle distance of 100 m). We assume a noise power N of $-99\,\mathrm{dBm}$, an SINR threshold of $\beta = 8\,\mathrm{dB}$ [13], and that $A = 3 \cdot 10^{-5}$, approximately matching the conditions in [30]. We set the transmit power to $P = 100\,\mathrm{mW}$, corresponding to 20 dBm. Only the rural scenario is evaluated, though we have verified that the Erlang approximation is valid for reasonable values of the shadowing standard deviation [8] in the urban case as well.

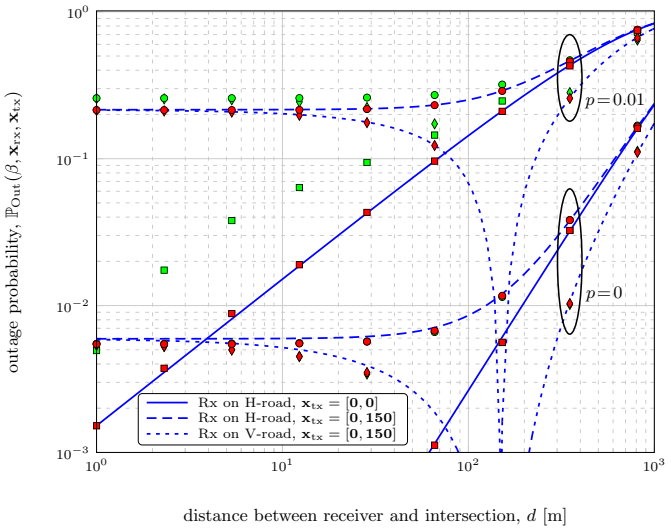

Fig. 2. Comparison of analytical (blue lines) and simulated (red markers) outage probability versus distance between receiver and intersection d, for different transmitter locations $\mathbf{x}_{\mathrm{tx}}$ as well as different Aloha transmit probabilities $p \in \{0, 0.01\}$. Green markers show results of SUMO simulation.

B. Outage Results

We show the outage for the analytical expressions, the numerical Monte Carlo simulations with random PPP and fading, and the SUMO simulations, for Aloha and CSMA/CA in Fig. 2 and Fig. 3, respectively.

[5]Note that the effects of a CSMA/CA MAC in an urban intersection can be evaluated following a similar approach

[6]The simulation was set up as follows: in SUMO version 0.31.0 we created four single-lane roads of 20 km and a traffic light in the center (default 4-arm intersection with 31 second green phase and 90 second cycle time). Flows on each lane was generated for 12,000 seconds with an arrival probability of 0.069 vehicles / second with a binomially distributed flow to approximate Poisson arrivals and a maximum speed of 70 km/h. After an initial simulation time of 2,000 seconds, snapshots of the 10,000 networks were stored and used to evaluate the outage probability. Data packets are always available and were transmitted according to the MAC protocol.

For Aloha, we observe an excellent match between the analytical expressions and the Monte Carlo simulations. In the absence of interferers ($p = 0$) the system achieves an outage probability of around 10% when the receiver and transmitter are spaced approximately 600 m apart, irrespective of the absolute position of transmitter and receiver. When p is increased to 0.01, these ranges reduce to around 60 m (when the transmitter is in the center of the intersection), or 70-80 m (when the transmitter is at $[0\,150]$). The outage probability increases slightly as the receiver gets closer to the intersection and sees more interferers. In the presence of interference ($p = 0.01$), the SUMO results yield a higher outage, which is mainly due to the clustering of vehicles near the intersection in the SUMO simulation. We also observe that as the distance between the receiver and the intersection increases, the agreement between the two spatial models becomes better in terms of outage probability, indicating that even though the PPP model fails in capturing the effect of traffic congestions it provides reasonable results for free-flow traffic. Although not further investigated here, clustering effects due to traffic congestions could be modeled by considering non-homogeneous PPPs with a higher intensity of vehicles close to the intersection, as was done in [1].

For CSMA, in order to evaluate the accuracy of the approximation introduced in Section III-A3, we start by comparing the analytically calculated outage probability to a simulation with 50,000 realizations of the fading parameters and the hard-core process induced by the dependent thinning resulting from the CSMA/CA scheme. This comparison can be seen in Fig. 3, which shows the analytical and simulated outage probability as a function of the distance between the receiver and the intersection for two different transmitter locations ($\mathbf{x}_{\mathrm{tx}} = [0, 0]$ and $\mathbf{x}_{\mathrm{tx}} = [0, 150]$), as well as two different CSMA/CA interference ranges $\delta \in \{500\,\mathrm{m}, 10000\,\mathrm{m}\}$. We observe better correspondence between SUMO simulation results and the analytical results than in the Aloha case: in CSMA/CA the physical clustering of vehicles is still present, but its impact is reduced due to the inherent properties of CSMA/CA, which counteracts the physical clustering by enforcing a distance of at least the interference range δ between active transmitters. We also note that when $\mathbf{x}_{\mathrm{tx}} = [0, 0]$, it is possible to compare Fig. 3 with Fig. 2. We note that for $\delta = 10000\,\mathrm{m}$, for a distance of 100 m between Rx and intersection, CSMA/CA has an outage probability of 0.003, while slotted Aloha is over 25 times worse, with an outage probability of 0.08.

C. Throughput Results

To further study the performance gains achieved by using CSMA/CA compared to slotted Aloha, we now look at both outage probability and throughput for a specific receiver and transmitter configuration. The configuration that we consider is $\mathbf{x}_{\mathrm{rx}} = [0\,0]^{\mathrm{T}}$ and $\mathbf{x}_{\mathrm{tx}} = [R_{\mathrm{comm}}\,0]^{\mathrm{T}}$. Note that for the slotted Aloha case this placement results in the worst possible throughput for a fixed $l_{\mathrm{E}}(\mathbf{x}_{\mathrm{tx}}, \mathbf{x}_{\mathrm{rx}})$. Fig. 4 and Fig. 5 show the outage probability and throughput as a function of the access probability $p_A(\mathbf{x}_{\mathrm{tx}})$, for two different values on $R_{\mathrm{comm}} \in \{100\,\mathrm{m}, 200\,\mathrm{m}\}$.

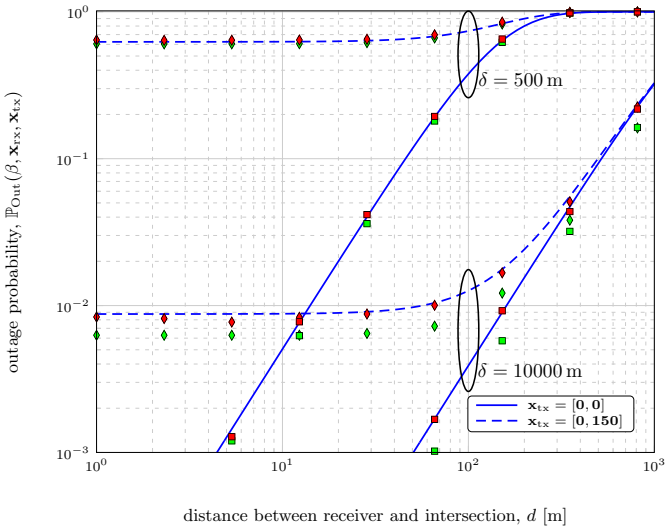

Fig. 3. Comparison of analytical (blue lines) and simulated (red markers) outage probability versus distance between receiver and intersection d, for different transmitter locations $\mathbf{x}_{\mathrm{tx}}$ as well as different CSMA/CA interference ranges $\delta \in \{500\,\mathrm{m}, 10\,\mathrm{km}\}$, which in the region where the access probability is constant, i.e., far away from the intersection, corresponds to $p_A = 0.1$ and $p_A = 0.005$, respectively. Green markers show results of SUMO simulation.

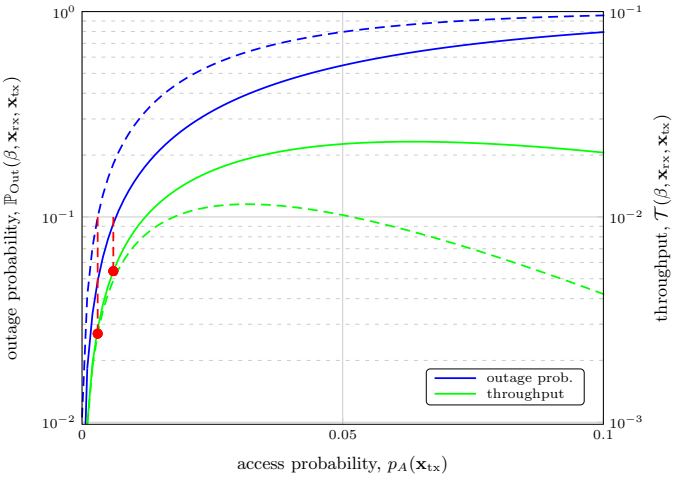

Fig. 4. Slotted Aloha outage probability $\mathbb{P}_{\mathrm{Out}}(\beta, \mathbf{x}_{\mathrm{rx}}, \mathbf{x}_{\mathrm{tx}})$ and throughput $\mathcal{T}(\beta, \mathbf{x}_{\mathrm{rx}}, \mathbf{x}_{\mathrm{tx}})$ as a function of the transmitter access probability $p_A(\mathbf{x}_{\mathrm{tx}})$. The receiver is located at $\mathbf{x}_{\mathrm{rx}} = [0, 0]$, and solid lines correspond to $R_{\mathrm{comm}} = 100\,\mathrm{m}$, while dashed lines correspond to $R_{\mathrm{comm}} = 200\,\mathrm{m}$. The red circles indicate the maximum throughput that is possible to achieve while guaranteeing that the outage probability is kept below the target value of 10 %.

For slotted Aloha (Fig. 4), we see that with an increase in $p_A(\mathbf{x}_{\mathrm{tx}})$, outage probability increases due to the presence of more interferers. The throughput first increases (due to more active transmitters) and then decreases (due to overwhelming amounts of interference), leading to an optimal value of $p_A(\mathbf{x}_{\mathrm{tx}})$. However, to guarantee a certain quality of service, one must also consider a guarantee on the outage probability. For instance, if we want to guarantee an outage probability of less than 10 % on the link when $R_{\mathrm{comm}} = 100\,\mathrm{m}$, the optimal value of $p_A(\mathbf{x}_{\mathrm{tx}}) \approx 0.006$, leading to a throughput of around 0.0055 bits per unit time and bandwidth.

For CSMA/CA (Fig. 5), a low access probability (i.e., large interference region) reduces the outage probability. Similar to

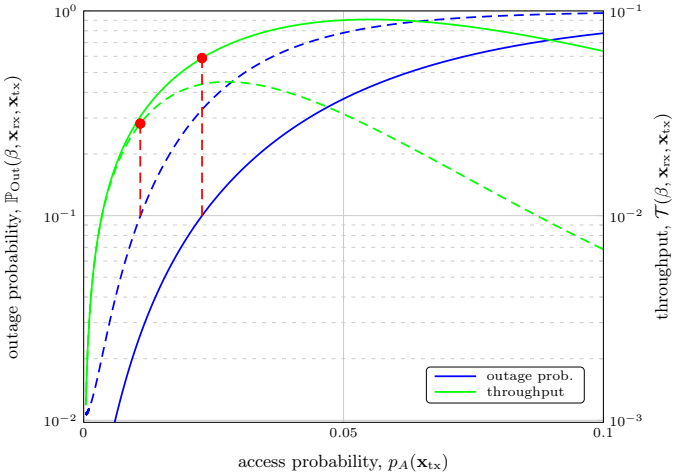

Fig. 5. CSMA/CA outage probability $\mathbb{P}_{\mathrm{Out}}(\beta, \mathbf{x}_{\mathrm{rx}}, \mathbf{x}_{\mathrm{tx}})$ and throughput $\mathcal{T}(\beta, \mathbf{x}_{\mathrm{rx}}, \mathbf{x}_{\mathrm{tx}})$ as a function of the transmitter access probability $p_A(\mathbf{x}_{\mathrm{tx}})$. The receiver is located at $\mathbf{x}_{\mathrm{rx}} = [-100, 0]$, and solid lines correspond to $R_{\mathrm{comm}} = 100\,\mathrm{m}$, while dashed lines correspond to $R_{\mathrm{comm}} = 200\,\mathrm{m}$. The red circles indicate the maximum throughput that is possible to achieve while guaranteeing that the outage probability is kept below the target outage probability of 10 %.

slotted Aloha, the throughput first increases with increased access probability and then decreases. To achieve an outage probability below 10 % when $R_{\mathrm{comm}} = 100\,\mathrm{m}$, the optimal value of $p_A(\mathbf{x}_{\mathrm{tx}}) \approx 0.023$ (corresponding to a interference range δ of about 1100 m), results in a throughput of about 0.059 bits per unit time and bandwidth. Hence, in this scenario, using CSMA/CA instead of slotted Aloha leads to more than a tenfold increase in the throughput for the same communication range. These results are congruent with general knowledge of CSMA/CA and slotted Aloha and indicate that the proposed framework can provide reasonable insights regarding communication performance.

VI. Conclusions

We have provided an overview of the dominant propagation properties of vehicular communication systems near intersections, for both rural and urban scenarios. Based on these properties, we proposed a procedure to analytically determine packet reception probabilities of individual transmissions as well throughput, mainly applicable to 802.11p communication. We find that the structure of the scenario, with two roads that cross, in combination with the CSMA/CA MAC leads to location-dependent packet reception probabilities and throughputs. We have applied this procedure to three case studies, relevant for vehicular applications. Based on these case studies, we found that the proposed procedure can capture the performance of a variety of realistic scenarios. Nevertheless, further evaluation is needed to assess the performance of the procedure in a wider variety of traffic scenarios (e.g., vehicle densities) and MAC parameters. We also found that the procedure is sensitive to model mismatch. In particular, the homogeneous PPP assumption fails to capture clustering of vehicles near the intersection, which is especially seen under Aloha. When the modeling assumptions are violated (e.g., different channel model, vehicle density, MAC protocol options), the analytical results may be overly optimistic or pessimistic, in which case the proposed procedure should be applied with a refined model. This is left for future work. In any case, the procedure can serve as a useful guide for communication system engineers, complementing simulations and experiments. Other possible avenues for future research include validation of the model against actual measurements, adoption of advanced MAC schemes as well as 5G D2D features.

Appendix A
Proof of Proposition 4

We use the procedure from Section III-C.

Step 1: The fading LTs for the interfering links from the H-road and the V-road can be expressed as $\mathcal{L}_{S_{\mathbf{x}}}(s) = 1/(1+s)$ and $\mathcal{L}_{S_{\mathrm{x}}}(s) = 1/(1+s\theta_V)^{k_V}$, respectively.

Step 2: According to Section III-A3 the intensity of the two PPPs $\Phi_{\mathrm{H}}^{\mathrm{MAC}}$ and $\Phi_{\mathrm{V}}^{\mathrm{MAC}}$ are $p\lambda_{\mathrm{H}}$ and $p\lambda_{\mathrm{V}}$, respectively.

Step 3: The LT of the interference for the two roads are derived in the following way. For the H-road, with interferers $\mathbf{x} \in \Phi_{\mathrm{H}}^{\mathrm{MAC}}$, the fading LT as well as the loss function are the same as in the rural intersection case. Following [38, eq. (13)], we can express the LT of the interference for a general α as

$$\mathcal{L}_{I_{\mathrm{H}}}(s) = \exp\left(-2p\lambda_{\mathrm{H}}\left(As\right)^{1/\alpha}\pi/\alpha\csc\left(\pi/\alpha\right)\right). \tag{21}$$

For the V-road we now have fading LT $\mathcal{L}_{S_{\mathrm{x}}}(s) = 1/(1+s\theta_V)^{k_V}$, intensity $p\lambda_{\mathrm{V}}$, and Manhattan loss function. Hence, using (8) we can write

$$\mathcal{L}_{I_V}(s) = \exp\left(-\int_{-\infty}^{\infty}\lambda_{\mathrm{V}}^{\mathrm{MAC}}(\mathbf{x}(z),\mathbf{x}_{\mathrm{tx}})(1-\mathcal{L}_{S_{\mathbf{x}}}(s\,l_{\mathrm{M}}(\mathbf{x}(z),\mathbf{x}_{\mathrm{rx}})))\mathrm{d}z\right) \tag{22}$$

$$= \exp\left(-p\lambda_{\mathrm{V}}\sum_{q=0}^{k_{\mathrm{V}}-1}\binom{k_{\mathrm{V}}}{q}\int_{-\infty}^{\infty}\frac{u^{\alpha q}b^{k_{\mathrm{V}}-q}}{(u^{\alpha}+b)^{k_{\mathrm{V}}}}\mathrm{d}u\right) \tag{23}$$

where we have invoked the Binomial Theorem and introduced variable changes $s\theta_{\mathrm{V}}A \to b$ and $d+|y| \to u$, where for points $\mathbf{x} \in \Phi_{\mathrm{V}}^{\mathrm{MAC}}$ the distance $\|\mathbf{x}_{\mathrm{rx}} - \mathbf{x}\|_1 = |x_{\mathrm{rx}}| + |y| = d + |y|$. For $q \geq 0$, $k_{\mathrm{V}} \geq q+1$, $b \geq 0$ and $d > 0$ the integral can be evaluated in closed form, and for a general α we can express the LT of the interference as

$$\mathcal{L}_{I_V}(s) = \exp\Bigg(-2p\lambda_{\mathrm{V}}\sum_{q=0}^{k_{\mathrm{V}}-1}\binom{k_{\mathrm{V}}}{q}\frac{1}{\alpha\Gamma\left[k_{\mathrm{V}}\right]}\left(\frac{As}{\theta_{\mathrm{V}}}\right)^{-q} \times\Gamma\left[\frac{1}{\alpha}+q\right]\Bigg(-\left(\frac{As}{\theta_{\mathrm{V}}}\right)^{-\frac{1}{\alpha}+q}\Gamma\left[-\frac{1}{\alpha}+k_{\mathrm{V}}-q\right] + d^{1+\alpha q}\,\Gamma\left[k_{\mathrm{V}}\right]{}_2F_1\left[k_{\mathrm{V}}, \frac{1}{\alpha}+q, 1+\frac{1}{\alpha}+q, -\frac{d^{\alpha}}{As\theta_{\mathrm{V}}}\right]\Bigg)\Bigg), \tag{24}$$

where ${}_2F_1$ is the regularized hypergeometric function. Note that for $\alpha = 2$ and $k_{\mathrm{V}} = \theta_{\mathrm{V}} = 1$ (i.e., exponential fading) this simplifies to

$$\mathcal{L}_{I_{\mathrm{V}}}(s)=\exp\left(-p\lambda_{\mathrm{V}}\sqrt{As}\left(\pi-2\arctan\left(\frac{d}{\sqrt{As}}\right)\right)\right), \quad (25)$$

and when $d\to 0$ we get $\mathcal{L}_{I_{\mathrm{V}}}(s)=\exp\left(-p\lambda_{\mathrm{V}}\pi\sqrt{As}\right)$.

Step 4: The fading on the useful link is characterized by its LT $\mathcal{L}_{S_0}(s)=1/(1+s\theta_0)^{k_0}$ and CCDF

$$\bar{F}_{S_0}(s)=e^{-s/\theta_0}\sum_{i=0}^{k_0-1}\frac{1}{i!\theta_0^i}s^i \quad (26)$$

Step 5: We now use the LTs of the interference from Step 3, and the CCDF of the fading from Step 4 to determine $\mathbb{P}(\beta,\mathbf{x}_{\mathrm{rx}},\mathbf{x}_{\mathrm{tx}})$ through (3). First using the CCDF, and evaluating it in the desired point, we can write

$$\begin{aligned}
&\bar{F}_{S_0}\left(\left(t_1+t_2+\tilde{N}\right)\tilde{\beta}\right)\\
&=e^{-\tilde{\beta}\left(t_1+t_2+\tilde{N}\right)/\theta_0}\sum_{i=0}^{k_0-1}\frac{1}{i!\theta_0^i}\left(\tilde{\beta}\right)^i\left(t_1+t_2+\tilde{N}\right)^i && (27)\\
&\overset{(a)}{=}e^{-\zeta\left(t_1+t_2+\tilde{N}\right)}\sum_{i=0}^{k_0-1}\frac{\zeta^i}{i!}\left(t_1+t_2+\tilde{N}\right)^i && (28)\\
&\overset{(b)}{=}e^{-\zeta\tilde{N}}\sum_{i=0}^{k_0-1}\sum_{j=0}^{i}\binom{i}{j}\frac{\zeta^i}{i!}e^{-\zeta t_1}(\tilde{N}+t_1)^j e^{-\zeta t_2}t_2^{i-j}, && (29)
\end{aligned}$$

where (a) involves the variable change $\zeta=\tilde{\beta}/\theta_0$ and (b) uses the Binomial Theorem. Due to the independence of the interference we can now use (29) to express the transform in (3) as

$$\mathbb{P}(\beta,\mathbf{x}_{\mathrm{rx}},\mathbf{x}_{\mathrm{tx}})=e^{-\frac{\zeta N}{P}}\sum_{i=0}^{k_0-1}\sum_{j=0}^{i}\binom{i}{j}\frac{\zeta^i}{i!}C^{(j)}D^{(i-j)}, \quad (30)$$

where

$$\begin{aligned}
C^{(j)}&=\int_0^{+\infty}e^{-\zeta t_1}(\tilde{N}+t_1)^j f_{I_{\mathrm{H}}}(t_1)\mathrm{d}t_1 && (31)\\
&=\sum_{n=0}^{j}\binom{j}{n}\tilde{N}^{j-n}\mathcal{L}[t_1^n f_{I_{\mathrm{H}}}(t_1)](\zeta) && (32)\\
&=\sum_{n=0}^{j}\binom{j}{n}\left(\frac{N}{P}\right)^{j-n}(-1)^n\frac{\mathrm{d}^n}{\mathrm{d}\zeta^n}\mathcal{L}_{I_{\mathrm{H}}}(\zeta) && (33)
\end{aligned}$$

and

$$\begin{aligned}
D^{(m)}&=\int_0^{+\infty}e^{-\zeta t_2}t_2^m f_{I_{\mathrm{V}}}(t_2)\mathrm{d}t_2 && (34)\\
&=\mathcal{L}[t_2^m f_{I_{\mathrm{V}}}(t_2)](\zeta) && (35)\\
&=(-1)^m\frac{\mathrm{d}^m}{\mathrm{d}\zeta^m}\mathcal{L}_{I_{\mathrm{V}}}(\zeta) && (36)
\end{aligned}$$

are obtained using the Laplace transform property $t^n f(t)\longleftrightarrow(-1)^n\frac{\mathrm{d}^n}{\mathrm{d}\zeta^n}\mathcal{L}[f(t)](\zeta)$. Note that (30) and (33) use the variable change $\tilde{N}=N/P$. Now using the results from Step 4, we can express the n^{th} derivative of the LT of the interference from the H-road as

$$\begin{aligned}
&\frac{\mathrm{d}^n}{\mathrm{d}\zeta^n}\mathcal{L}_{I_{\mathrm{H}}}(\zeta)\\
&=e^{-\kappa\sqrt{\zeta}}\zeta^{-n}\sum_{l=0}^{n}\sum_{m=0}^{l}\frac{(-1)^m\left(-\kappa\sqrt{\zeta}\right)^l\left(\frac{2-m+l-2n}{2}\right)_n}{m!\,(-m+l)!} && (37)
\end{aligned}$$

where $(\cdot)_n$ is the Pochhammer symbol and $\kappa=2p\lambda_{\mathrm{H}}(A)^{1/\alpha}\pi/\alpha\csc(\pi/\alpha)$. For the V-road, there is no general compact expression for the n^{th} derivative of $\mathcal{L}_{I_{\mathrm{V}}}(\zeta)$, but an explicit expression can in principle be calculated for any n, k_{V} and θ_{V}. Thus, inserting (24) in (36) concludes the proof.

Appendix B
Proof of Proposition 5

We use the procedure from Section III-C.

Step 1: The fading LT for the interfering links can be expressed as $\mathcal{L}_{S_{\mathbf{x}}}(s)=1/(1+s)$.

Step 2: According to Section III-A3, the intensity of the two PPPs $\Phi_{\mathrm{H}}^{\mathrm{MAC}}$ and $\Phi_{\mathrm{V}}^{\mathrm{MAC}}$ are for this case also a function of the transmitter location $\mathbf{x}_{\mathrm{tx}}$. Using (10) we can express the intensity for the H-road as

$$\begin{aligned}
&\lambda_{\mathrm{H}}^{\mathrm{MAC}}\left([x,0]^{\mathrm{T}},\mathbf{x}_{\mathrm{tx}}\right) && (38)\\
&=\begin{cases}\frac{1-\exp(-2\delta\lambda_{\mathrm{H}})}{2\delta} & x\in\mathcal{R}_1\\ \frac{1-\exp\left(-2\delta\lambda_{\mathrm{H}}-2\sqrt{\delta^2-x^2}\lambda_{\mathrm{V}}\right)\lambda_{\mathrm{H}}}{2\delta\lambda_{\mathrm{H}}+2\sqrt{\delta^2-x^2}\lambda_{\mathrm{V}}} & x\in\mathcal{R}_2\\ 0 & \text{else}\end{cases}
\end{aligned}$$

in which $\mathcal{R}_1=\{x\,|\,|x|>\delta \text{ and } \sqrt{(x-x_{\mathrm{tx}})^2+y_{\mathrm{tx}}^2}>\delta\}$ and $\mathcal{R}_2=\{x\,|\,|x|\le\delta \text{ and } \sqrt{(x-x_{\mathrm{tx}})^2+y_{\mathrm{tx}}^2}>\delta\}$. Similarly for the V-road,

$$\begin{aligned}
&\lambda_{\mathrm{V}}^{\mathrm{MAC}}\left([0,y]^{\mathrm{T}},\mathbf{x}_{\mathrm{tx}}\right) && (39)\\
&=\begin{cases}\frac{1-\exp(-2\delta\lambda_{\mathrm{V}})}{2\delta} & y\in\mathcal{R}_3\\ \frac{1-\exp\left(-2\delta\lambda_{\mathrm{V}}-2\sqrt{\delta^2-y^2}\lambda_{\mathrm{H}}\right)\lambda_{\mathrm{V}}}{2\delta\lambda_{\mathrm{V}}+2\sqrt{\delta^2-y^2}\lambda_{\mathrm{H}}} & y\in\mathcal{R}_4\\ 0 & \text{else}\end{cases}
\end{aligned}$$

in which $\mathcal{R}_3=\{y\,|\,|y|>\delta \text{ and } \sqrt{(y-y_{\mathrm{tx}})^2+x_{\mathrm{tx}}^2}>\delta\}$ and $\mathcal{R}_4=\{y\,|\,|y|\le\delta \text{ and } \sqrt{(y-y_{\mathrm{tx}})^2+x_{\mathrm{tx}}^2}>\delta\}$.

Step 3: Using (8), the LT of the interference for the H- and V- road can be expressed as

$$\mathcal{L}_{I_{\mathrm{H}}}(s)=\exp\left(-\int_{-\infty}^{+\infty}\frac{\lambda_{\mathrm{H}}^{\mathrm{MAC}}\left([x,0]^{\mathrm{T}},\mathbf{x}_{\mathrm{tx}}\right)}{1+|x_{\mathrm{rx}}-x|^{\alpha}/As}\mathrm{d}x\right) \quad (40)$$

and

$$\mathcal{L}_{I_{\mathrm{V}}}(s)=\exp\left(-\int_{-\infty}^{+\infty}\frac{\lambda_{\mathrm{V}}^{\mathrm{MAC}}\left([0,y]^{\mathrm{T}},\mathbf{x}_{\mathrm{tx}}\right)}{1+\left\|[x_{\mathrm{rx}},-y]^{\mathrm{T}}\right\|_2^{\alpha}/As}\mathrm{d}y\right) \quad (41)$$

Step 4: The fading on the useful link is characterized by its LT $\mathcal{L}_{S_0}(s)=1/(1+s)$ and CCDF $\bar{F}_{S_0}(s)=\exp(-s)$.

Step 5: By applying a location-dependent thinning, we approximate the interference from the H- and V-road as independent. As the fading on the useful link is exponential (i.e.,

$S_0 \sim E(1,1)$), we can express the packet reception probability as $\mathbb{P}(\beta, \mathbf{x}_{\rm rx}, \mathbf{x}_{\rm tx}) = e^{-\tilde{N}\tilde{\beta}} \mathcal{L}_{I_{\rm H}}\left(\tilde{\beta}\right) \mathcal{L}_{I_{\rm V}}\left(\tilde{\beta}\right)$. Using the results from Step 3, and the variable change $\tilde{N} = N/P$, we can for the particular value of $\alpha = 2$ finally obtain (18). Note that for a general transmitter location $\mathbf{x}_{\rm tx}$, we are not able to evaluate the integrals in (40) and (41) in closed form, but have to resort to numerical evaluation.

REFERENCES

[1] E. Steinmetz, M. Wildemeersch, T. Q.S. Quek, and H. Wymeersch, "A Stochastic Geometry Model for Vehicular Communication near Intersections," in *IEEE Global Communications Conference (GLOBECOM)*, Dec. 2015.

[2] H. Hartenstein and K. P. Laberteaux, "A tutorial survey on vehicular ad hoc networks," *IEEE Communications Magazine*, vol. 46, no. 6, pp. 164–171, Jun. 2008.

[3] P. Papadimitratos, A. La Fortelle, K. Evenssen, R. Brignolo, and S. Cosenza, "Vehicular Communication Systems: Enabling Technologies, Applications, and Future Outlook on Intelligent Transportation," *IEEE Communications Magazine*, vol. 47, no. 11, pp. 84–95, Nov. 2009.

[4] G. Araniti, C. Campolo, M. Condoluci, A. Iera, and A. Molinaro, "LTE for vehicular networking: A survey," *IEEE Communications Magazine*, vol. 51, no. 5, pp. 148–157, May 2013.

[5] R. Johri, J. Rao, H. Yu, and H. Zhang, "A multi-scale spatiotemporal perspective of connected and automated vehicles: Applications and wireless networking," *IEEE Intelligent Transportation Systems Magazine*, vol. 8, no. 2, pp. 65–73, Summer 2016.

[6] J. Santa, R. Toledo-Moreo, M. A. Zamora-Izquierdo, B. Úbeda, and A. F. Gómez-Skarmeta, "An analysis of communication and navigation issues in collision avoidance support systems," *Transportation Research Part C: Emerging Technologies*, vol. 18, no. 3, pp. 351–366, Jun. 2010.

[7] C. F. Mecklenbrauker, A. F. Molisch, J. Karedal, F. Tufvesson, A. Paier, L. Bernado, T. Zemen, O. Klemp, and N. Czink, "Vehicular Channel Characterization and Its Implications for Wireless System Design and Performance," *Proceedings of the IEEE*, vol. 99, no. 7, pp. 1189–1212, Jul. 2011.

[8] T. Abbas, A. Thiel, T. Zemen, C. F. Mecklenbrauker, and F. Tufvesson, "Validation of a non-line-of-sight path-loss model for V2V communications at street intersections," in *International Conference on ITS Telecommunications (ITST)*, Nov. 2013, pp. 198–203.

[9] T. Mangel, O. Klemp, and H. Hartenstein, "5.9 GHz inter-vehicle communication at intersections: a validated non-line-of-sight path-loss and fading model," *EURASIP Journal on Wireless Communications and Networking*, vol. 2011, no. 1, pp. 1–11, Nov. 2011.

[10] A. Moller, J. Nuckelt, D. M. Rose, and T. Kurner, "Physical layer performance comparison of lte and ieee 802.11p for vehicular communication in an urban nlos scenario," in *2014 IEEE 80th Vehicular Technology Conference (VTC2014-Fall)*, Sept 2014, pp. 1–5.

[11] C. Sommer, S. Joerer, M. Segata, O. K. Tonguz, R. L. Cigno, and F. Dressler, "How shadowing hurts vehicular communications and how dynamic beaconing can help," *IEEE Transactions on Mobile Computing*, vol. 14, no. 7, pp. 1411–1421, July 2015.

[12] H. Tchouankem, T. Zinchenko, and H. Schumacher, "Impact of buildings on vehicle-to-vehicle communication at urban intersections," in *2015 12th Annual IEEE Consumer Communications and Networking Conference (CCNC)*, Jan 2015, pp. 206–212.

[13] K. Sjöberg, "Medium Access Control for Vehicular Ad Hoc Networks," Ph.D. dissertation, Chalmers University of Technology, 2013.

[14] M. Haenggi and R. K. Ganti, "Interference in Large Wireless Networks," *Foundations and Trends in Networking*, vol. 3, no. 2, pp. 127–248, 2008.

[15] R. K. Ganti and M. Haenggi, "Interference and Outage in Clustered Wireless Ad Hoc Networks," *IEEE Transactions on Information Theory*, vol. 55, no. 9, pp. 4067–4086, Sep. 2009.

[16] N. Deng, W. Zhou, and M. Haenggi, "The Ginibre Point Process as a Model for Wireless Networks With Repulsion," *IEEE Transactions on Wireless Communications*, vol. 14, no. 1, pp. 107–121, Jan. 2015.

[17] A. Hunter, J. Andrews, and S. Weber, "Transmission capacity of ad hoc networks with spatial diversity," *IEEE Transactions on Wireless Communications*, vol. 7, no. 12, pp. 5058–5071, Dec. 2008.

[18] R. W. Heath, M. Kountouris, and T. Bai, "Modeling Heterogeneous Network Interference Using Poisson Point Processes," *IEEE Transactions on Signal Processing*, vol. 61, no. 16, pp. 4114–4126, Aug. 2013.

[19] B. Błaszczyszyn and H. Keeler, "Equivalence and comparison of heterogeneous cellular networks," in *IEEE 24th International Symposium on Personal, Indoor and Mobile Radio Communications (PIMRC Workshops)*, Sep. 2013, pp. 153–157.

[20] Y. Jeong, J. W. Chong, H. Shin, and M. Z. Win, "Intervehicle Communication: Cox-Fox Modeling," *IEEE Journal on Selected Areas in Communications*, vol. 31, no. 9, pp. 418–433, Sep. 2013.

[21] Z. Tong, H. Lu, M. Haenggi, and C. Poellabauer, "A Stochastic Geometry Approach to the Modeling of DSRC for Vehicular Safety Communication," *IEEE Transactions on Intelligent Transportation Systems*, vol. 17, no. 5, pp. 1448–1458, May 2016.

[22] B. Błaszczyszyn, P. Mühlethaler, and Y. Toor, "Performance of MAC protocols in linear VANETs under different attenuation and fading conditions," in *IEEE Conference on Intelligent Transportation Systems*, Oct. 2009, pp. 1–6.

[23] ——, "Stochastic analysis of Aloha in vehicular ad hoc networks," *Annales des Télécommunications*, vol. 68, no. 1, pp. 95–106, Jun. 2013.

[24] T. V. Nguyen, F. Baccelli, K. Zhu, S. Subramanian, and X. Wu, "A performance analysis of CSMA based broadcast protocol in VANETs," in *Proceedings IEEE INFOCOM*, April 2013, pp. 2805–2813.

[25] M. J. Farooq, H. ElSawy, and M. Alouini, "A stochastic geometry model for multi-hop highway vehicular communication," *IEEE Transactions on Wireless Communications*, vol. 15, no. 3, pp. 2276–2291, March 2016.

[26] E. Steinmetz, R. Hult, G. R. de Campos, M. Wildemeersch, P. Falcone, and H. Wymeersch, "Communication analysis for centralized intersection crossing coordination," in *International Symposium on Wireless Communications Systems (ISWCS)*, Aug. 2014, pp. 813–818.

[27] M. Abdulla, E. Steinmetz, and H. Wymeersch, "Vehicle-to-vehicle communications with urban intersection path loss models," in *IEEE Globecom Workshops (GC Wkshps)*, Dec 2016.

[28] SUMO, "Simulation of Urban MObility," dlr.de/ts/sumo.

[29] T. Abbas, K. Sjöberg, J. Karedal, and F. Tufvesson, "A measurement based shadow fading model for vehicle-to-vehicle network simulations," *International Journal of Antennas and Propagation*, vol. 2015, 2015, Article ID 190607, 12 pages, 2015.

[30] J. Karedal, N. Czink, A. Paier, F. Tufvesson, and A. F. Molisch, "Path Loss Modeling for Vehicle-to-Vehicle Communications," *IEEE Transactions on Vehicular Technology*, vol. 60, no. 1, pp. 323–328, Jan. 2011.

[31] FP6 IST Project WINNER II, Deliverable 1.1.2 V1.2, "WINNER II Channel Models," Sep. 2007. [Online]. Available: http://www.cept.org/files/1050/documents/winner2%20-%20final%20report.pdf

[32] A. Goldsmith, *Wireless Communications*. Cambridge University Press, 2005.

[33] L. Cheng, B. Henty, D. Stancil, F. Bai, and P. Mudalige, "Mobile Vehicle-to-Vehicle Narrow-Band Channel Measurement and Characterization of the 5.9 GHz Dedicated Short Range Communication (DSRC) Frequency Band," *IEEE Journal on Selected Areas in Communications*, vol. 25, no. 8, pp. 1501–1516, Oct. 2007.

[34] M. Haenggi, "Mean interference in hard-core wireless networks," *IEEE Communications Letters*, vol. 15, no. 8, pp. 792–794, Aug. 2011.

[35] C. Abou-Rjeily and M. Bkassiny, "On the achievable diversity orders over non-severely faded lognormal channels," *IEEE Communications Letters*, vol. 14, no. 8, pp. 695–697, Aug. 2010.

[36] S. R. Cho and W. Choi, "Energy-efficient repulsive cell activation for heterogeneous cellular networks," *IEEE Journal on Selected Areas in Communications*, vol. 31, no. 5, pp. 870–882, May 2013.

[37] E. Steinmetz, M. Wildemeersch, and H. Wymeersch, "WiP abstract: Reception Probability Model for Vehicular Ad-Hoc Networks in the Vicinity of Intersections," in *ACM/IEEE International Conference on Cyber-Physical Systems (ICCPS)*, Apr. 2014, pp. 223–223.

[38] M. Haenggi, "Outage, local throughput, and capacity of random wireless networks," *IEEE Transactions on Wireless Communications*, vol. 8, no. 8, pp. 4350–4359, 2009.

Erik Steinmetz received his M.Sc. in Electrical Engineering, and Ph.D. in Signals and Systems from Chalmers University of Technology, in 2009 and 2019, respectively. Currently, he is a researcher with RISE Research Institutes of Sweden. His research interests include positioning, sensor fusion, communication and controls applied within the fields of intelligent vehicles and cooperative automated driving.

Matthias Wildemeersch received the M.Sc. degree in electromechanical engineering from Ghent University, Belgium, and the Ph.D. degree in electrical engineering at the University of Twente, The Netherlands. He gained professional experience at the Joint Research Centre of the European Commission, the Agency for Science, Technology and Research (A*STAR) in Singapore, and the Singapore University of Technology and Design (SUTD). Currently, he is a research scholar at the International Institute for Applied Systems Analysis (IIASA), where his work broadly covers the dynamical behavior of multi-agent networks. His research interests span various aspects of decision making, applying tools from mathematical economics, control, and stochastic optimization.

Tony Q.S. Quek (S'98-M'08-SM'12-F'17) received the B.E. and M.E. degrees in Electrical and Electronics Engineering from Tokyo Institute of Technology, Tokyo, Japan, respectively. At Massachusetts Institute of Technology, he earned the Ph.D. in Electrical Engineering and Computer Science. Currently, he is a tenured Associate Professor with the Singapore University of Technology and Design (SUTD). His main research interests are the application of mathematical, optimization, and statistical theories to communication, networking, signal processing, and resource allocation problems.

Henk Wymeersch (S'99, M'05) is a Professor with the Department of Electrical Engineering at Chalmers University of Technology, Sweden. Prior to joining Chalmers, he was a postdoctoral researcher from 2005 until 2009 with the Laboratory for Information and Decision Systems at the Massachusetts Institute of Technology. Henk Wymeersch obtained the Ph.D. degree in Electrical Engineering/Applied sciences in 2005 from Ghent University, Belgium. His current research interests include cooperative systems and intelligent transportation.